Supporting Information

Chemically Programmed Ultrahigh Density Two Dimensional Semiconductor Superlattice Array

Narayan Pradhan[1,3], Somobrata Acharya[2,3], Katsuhiko Ariga[2], Niladri S. Karan[3], D. D. Sarma[3,4], Yoshiki Wada[2], Shlomo Efrima[1] and Yuval Golan[5]*

[1]Department of Chemistry; Ben-Gurion University of the Negev, Beer-Sheva, ISRAEL 84105

[2]World Premier International (WPI) Research Center for Materials Nanoarchitectonics (MANA), National Institute for Materials Science (NIMS), 1-1 Namiki, Tsukuba, Ibaraki, 305-0044, JAPAN

[3]Centre for Advanced Materials, Indian Association for the Cultivation of Science, Kolkata 700032, INDIA

[4]Solid State and Structural Chemistry Unit & Centre for Condensed Matter Theory, Indian Institute of Science, Bangalore 560012, INDIA

[5]Department of Materials Engineering and Ilse Katz Institute for Meso and Nanoscale Science and Technology, Ben-Gurion University of the Negev, Beer-Sheva, ISRAEL 84105

Synthesis of ZnS rods

Octadecylamine (Fluka), ODA 97% pure, o-ethylxantic acid and zinc perchlorate hexahydrate 96% pure were purchased from Aldrich and used as received. Zinc-ethylxanthate was prepared by dissolving 3.00 g o-ethylxantic acid in methanol and adding 3.48 g of zinc perchlorate hexahydrate in methanol under continuous stirring. The mixture forms yellow white precipitate indicating salt formation. The salt was washed 3 times in methanol and dried in air before use. ODA-coated ZnS nanorods were prepared by dissolving 0.08g of zinc-ethylxanthate in 1.53g of molten ODA at a temperature of 100-105°C under nitrogen atmosphere. After 5 minutes, the temperature was increased to 130°C and annealed for 8 minutes. The reaction temperature was cooled down to 50°C and the ZnS nanorods were collected in methanol. Excess ligands were washed out by centrifuging and washing in methanol.

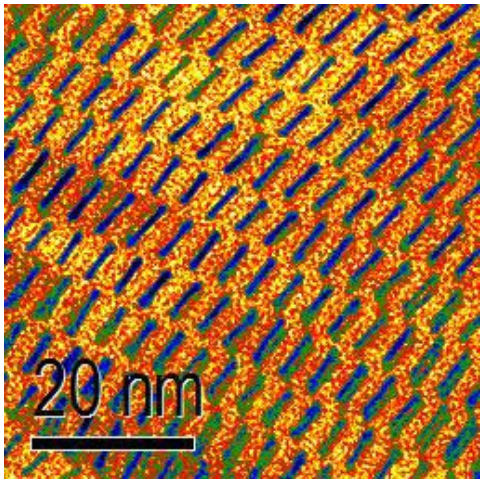

Figure 1. TEM image of 2D supercrystalline assembly of 1.2 nm x 5 nm ZnS rods capped by ODA [References: (a) Pradhan, N.; Efrima, S. *J. Phys. Chem. B.* **2004**, *108,* 11964. (b) Acharya, S.; Efrima, S. *J. Am. Chem. Soc*. **2005**, *127*, 3486].

Synthesis of CdS rods

Cadmium hexadecylxanthate (0.13 g) was added to molten hexadecylamine (HDA), 2 g, purchased from Aldrich, >98% purity) at 60 °C with continuous stirring under N_2. When clear yellow color appears, the temperature was increased to 90 °C, and after 30 min, the temperature was increased further to 130 °C and annealed for 1 h to complete the reaction. Subsequently, the temperature was slowly decreased to 50 °C, and methanol was added for flocculation.

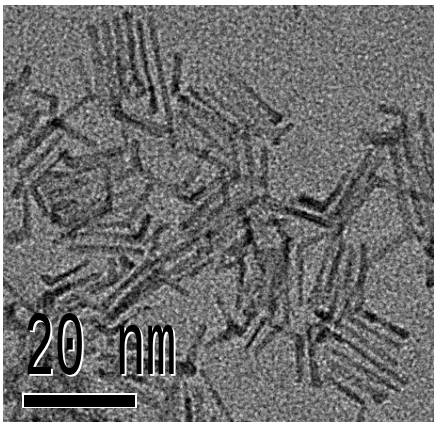

Figure 2. The reference 1.7 nm wide, 15-40 nm long CdS rods developed in wurtzite phase [Reference: Acharya, S.; Patla, I.; Kost, J.; Efrima, S.; Golan, Y. *J. Am. Chem. Soc.* **2006**, 128, 9294]. The optical absorption (figure 14 of S.I.) and emission spectra (figure 3a of manuscript) from these nanorods are compared with the (-ZnS-CdS-ZnS)n superlattice wires as reference sample.

Synthesis of (-ZnS-CdS-ZnS) heterostructures

ODA-coated ZnS nanorods were prepared by dissolving 0.08g of zinc-ethylxanthate in 1.53g of molten ODA at a temperature of 100-105°C under nitrogen atmosphere. After 5 minutes, the temperature was increased to 130°C and annealed for 8 minutes (reaction 1). The reaction temperature was cooled down to 70°C, where the Cd-xanthate precursor is added. Typically 0.9g melted ODA at taken 70°C in a separate text tube (reaction 2), where 3.04×10^{-5} moles Cd-hexadecylxanthate added and annealed for 5 minutes. The reaction 2 is added to reaction 1 in one shot with vigorous stirring at 70 °C. The temperature was gradually increased to 160°C and annealing was carried out for 1h Finally the temperature was reduced to 70°C and flocculated with methanol, centrifuged and redispersed in solvents like dichloromethane, toluene etc. High-resolution transmission electron microscopy (HRTEM), HREELS, HAADF, EDS was performed by using a JEOL-JEM2000 operating at 200 kV. The optical spectra were measured using JASCO V570 for UV-vis; pulsed laser source with CCD detector and Fluorolog 3, Jobin Yvon for PL measurements.

Alternative Synthesis route 1: Design (ZnS-CdS-ZnS)n superlattices after purification of ZnS nanorods

The ZnS rods have been prepared using Zn-ethayl xanthate in Hexadecylamine (HDA) as liganding solvent. Typically 0.08 g of zinc-ethylxanthate is added to 1.6 g of molten HDA at a temperature of 110°C under nitrogen atmosphere. The resultant ZnS rods were harvested after repetitive purification using with methanol as nonsolvent. The resultant rods were dried in air before use. The purified rods (half) are dissolved again in HDA and $1/10^{th}$ molar concentration of Cd-hexadecylxanthate injected at 70°C to synthesize CdS-ZnS heterostructure. The resultant heterostruture salt was washed repetitively in methanol and dried in air before use.

Alternative Synthesis route 2: Design (ZnS-CdS-ZnS)n superlattices using different precursor molecules

The ZnS rods/wire mixture has been prepared using Zn-diethyldithiocarbamate in HDA as liganding solvent. Typically 0.1 g of Zn-diethyldithiocarbamate is added to 2.5 g of molten HDA at a temperature of 120°C under nitrogen atmosphere. Cd-diethyldithiocarbamate (0.02g in 0.6g HDA) was injected at temperature of 110 ^{o}C with continuous stirring under N_2. The resultant mixture was annealed for 40 minutes with continuous stirring under N_2. Subsequently, the temperature was slowly reduced to 70 °C, and methanol was added for flocculation of the heterowires.

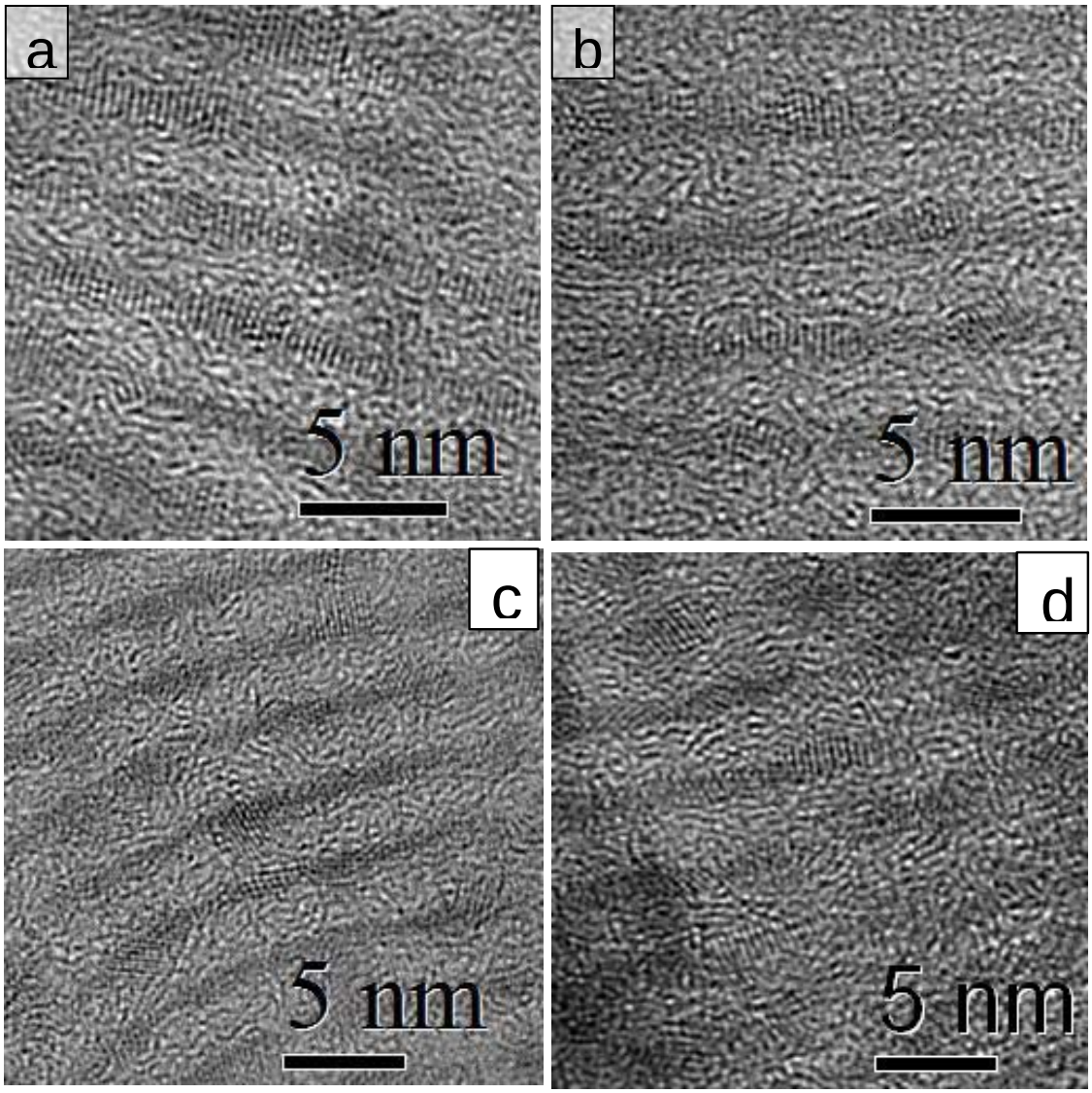

Figure 3. High resolution TEM images of the superlattice assembly demonstrating novel composition of alternative ZnS-CdS materials. The diameter of the ZnS units are 1.2 nm, the same as ZnS rods as shown in figure 1a of the supporting information. A periodic repeat unit of CdS bulges with little larger diameter around or less than 2 nm are observed demonstrating formation of dissimilar materials at the tips of ZnS rods forming the superlattice.

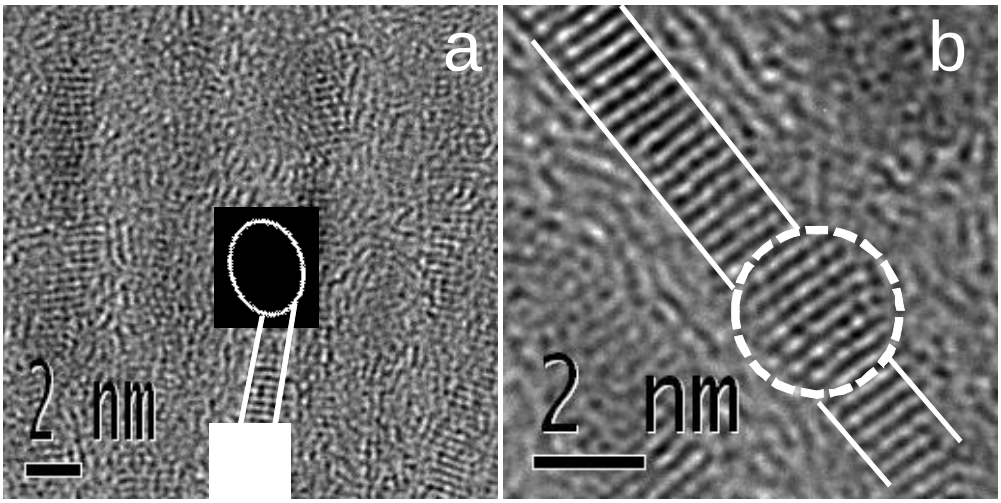

Figure 4. The HRTEM of ZnS-CdS regions. (a) CdS prolates with (10.0) wurtzite modifications. (b) CdS regions corresponding to (00.2) planes of wurtzite CdS forming a continuous lattice planes of $(00.2)_{ZnS}$ and $(00.2)_{CdS}$ perpendicular to the long axes of the superlattice wires. The $(00.2)_{ZnS}$ planes are always observed lying perpendicular to the length of the superlattice wire indicating the ZnS *c*-axis parallel to the long axis of the wires.

Structural Characterizations of (-ZnS-CdS-ZnS)n heterowires:

A. EDS analysis from different regions of (ZnS-CdS-ZnS)n superlattice wires

Table 1. EDS Elemental analysis carried out in the TEM of atomic compositions by selective area EDS. The ratio "Zn: S: Cd" indicates the atomic composition of Zinc, Sulfur and Cadmium from selected regions within the TEM grid.

Regions	Elements	Atom %	Zn:S:Cd
1	S	40.56	4:6:1
	Zn	36.60	
	Cd	7.85	
2	S	51.59	6:6:1

	Zn	54.32	
	Cd	9.08	
3	S	55.27	5:8:1
	Zn	37.99	
	Cd	6.74	
4	S	54.18	4:4:1
	Zn	36.42	
	Cd	9.40	
5	S	53.8	4:6:1
	Zn	37.9	
	Cd	8.3	

B. FET analysis from different regions of (ZnS-CdS-ZnS)n superlattice wires

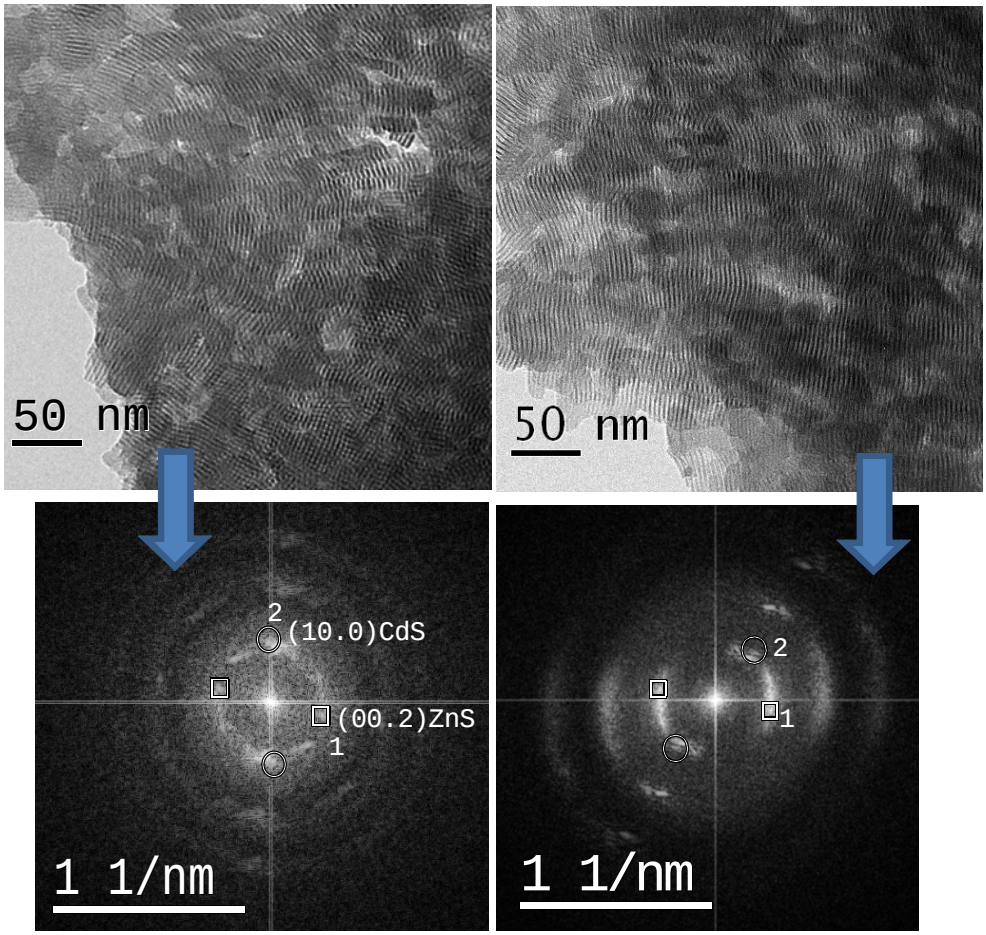

Figure 5. (Top) Low resolution TEM images of the (-ZnS-CdS-ZnS-)n assembly demonstrating large area parallel superlattice assemblies. (Bottom) FET of superlattices

taken from the corresponding entire frame of low resolution TEM images. Spot 1 corresponds to d-spacings of 0.32 nm corresponding to the $(00.2)_{ZnSWZ}$ phase and spot 2 corresponds to d-spacings of 0.35 nm corresponding to the $(10.0)_{CdSWZ}$ phase.

C. EELS analysis from different regions of (ZnS-CdS-ZnS)n superlattice wires

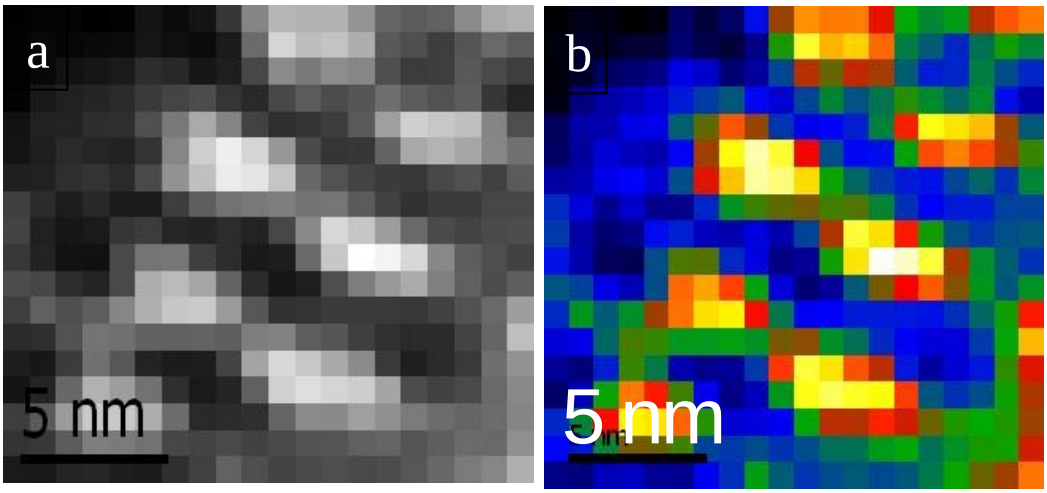

Figure 6. (a) Original spatially resolved nanoprobe electron energy loss spectroscopy (EELS) image of the superlattice wires showing a significant contrast difference at a separation of ~5 nm consistent with the repeat unit along the wire length. (b) The original image is color coded with lighter yellow-white are Zn rich regions and light-green are Cd rich regions; brighter colors indicate S regions.

D. Z-contrast image analysis from different regions of (ZnS-CdS-ZnS)n superlattice wires

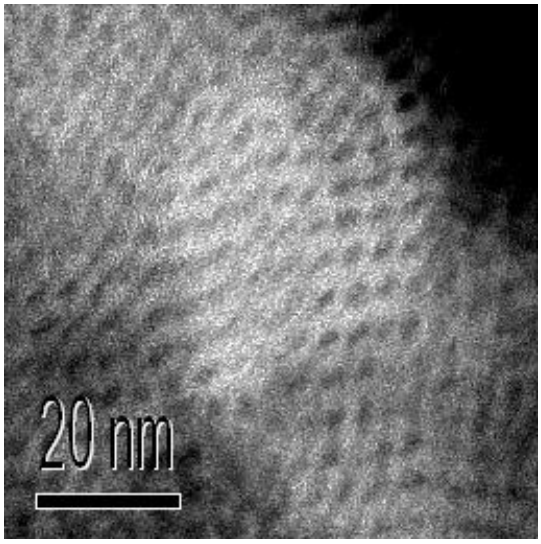

Figure 7. The Z-contrast imaging by high angular annular bright-field detector (HAADF) reveals significant contrast differences between CdS and ZnS regions, where the heavier CdS results brighter regions at 5 nm periodicity.

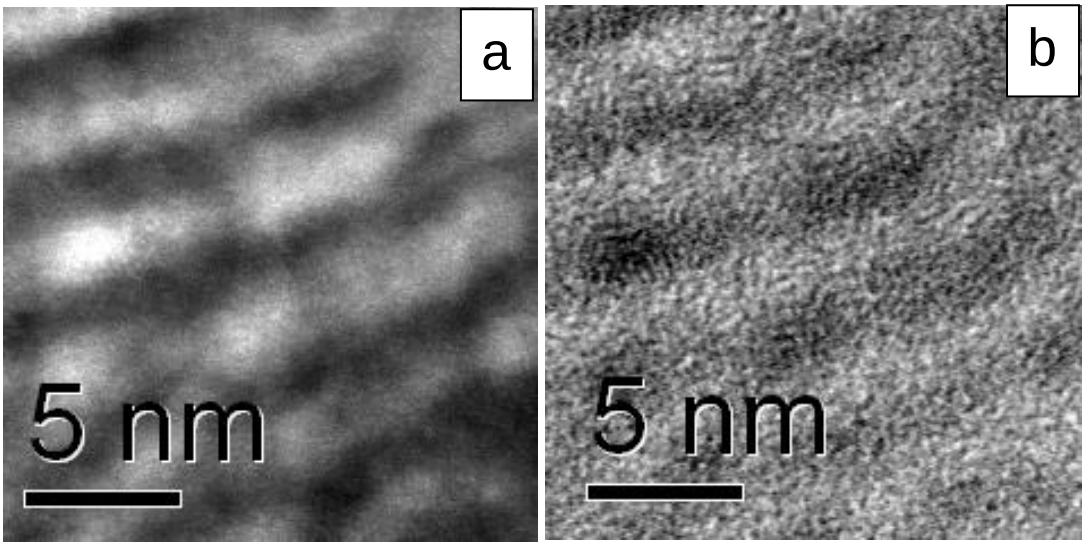

Figure 8. High resolution Z-contrast (a) dark field and (b) bright field images from an area of the superlattice showing opposite contrast difference between CdS and ZnS regions at 5 nm periodicity.

E. EELS line scan profile analysis from different regions of (ZnS-CdS-ZnS)n superlattice wires

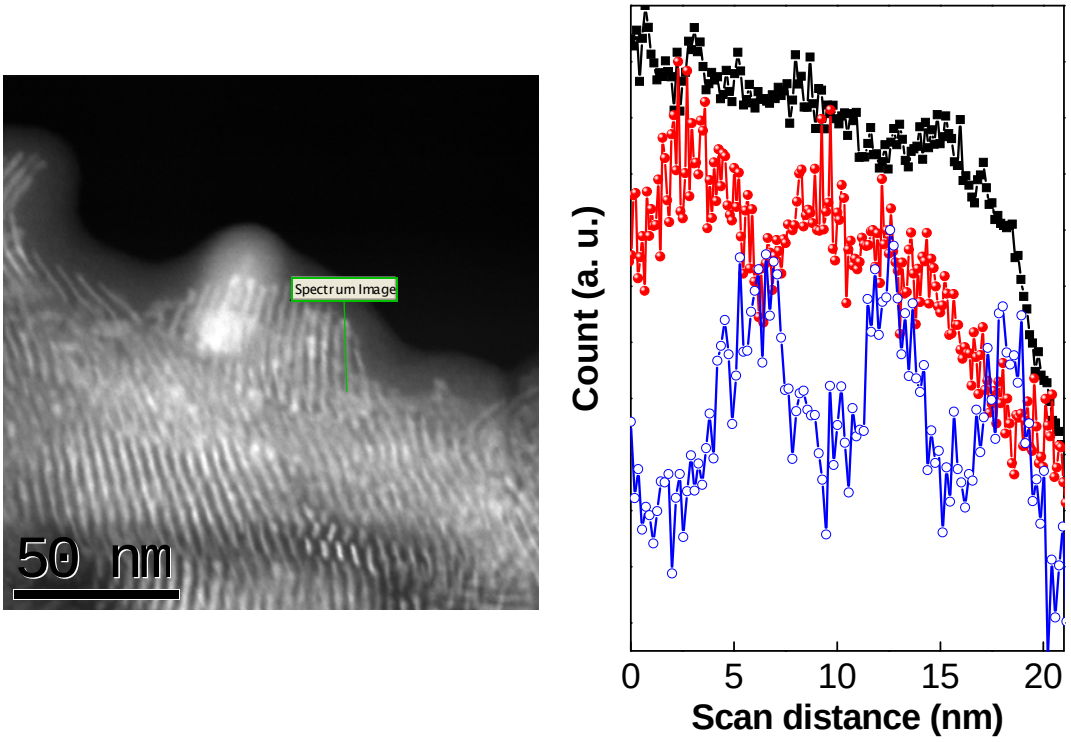

Figure 9. EELS line scan profile along a superlattice wire showing the composition variation at each 5 nm repeat distance. Left panel; the place where from the scanning has been performed, with the marked line indicate the specific wire. Right panel shows the elemental mapping with the Zn regions (red curve) extends through 5 nm regions, the Cd trace (blue curve) appears at each 5-6 nm repeat units, while the S (black curve) is detected throughout. The partial overlap of Zn and Cd peaks could indicate that the junctions might not be sharp, although the spatial resolution of EELS might prevent such direct conclusion.

F. Selected Area Electron Diffraction (SAED) analysis from of (ZnS-CdS-ZnS)n superlattice wires

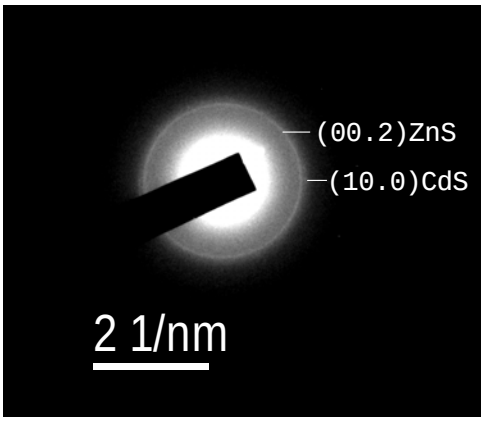

Figure 10. The SAED patterns obtained from the (-ZnS-CdS-ZnS-)n superlattice assembly showing wurtzite structure with $(00.2)_{ZnS}$ and $(10.0)_{CdS}$ diffraction rings, in line with the inter-planer distances of 0.32 nm and 0.35 nm of bulk wurtzite ZnS (JCPDS 36-1450) and CdS (JCPDS 41-1049). The strong intensity of the (002) reflection indicates a preferred orientation in which the wires are oriented with the [002] crystallographic axis.

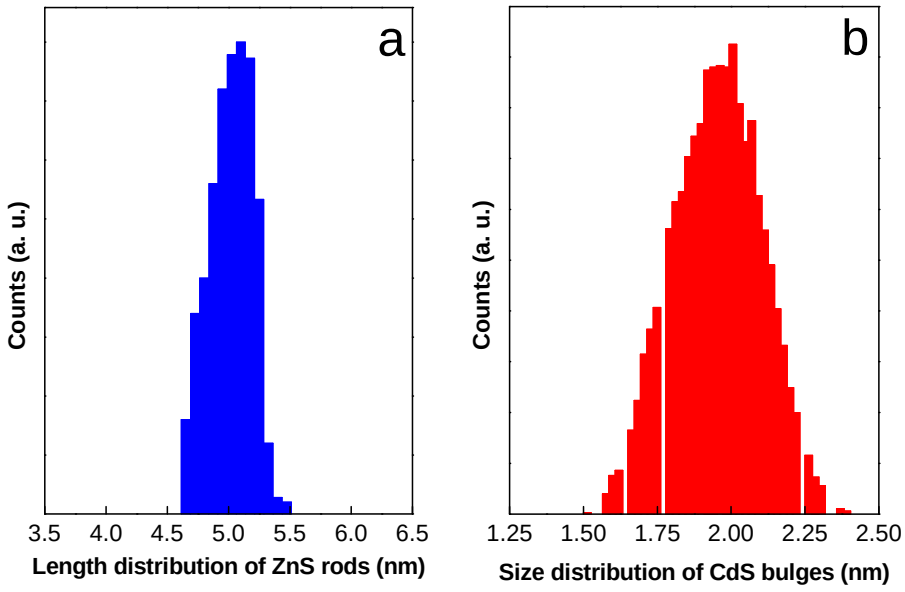

Figure 11. Statistical distribution of (a) the length of ZnS blocks which offers the barrier widths and (b) the sizes of the CdS bulges which offers the well widths.

G. Statistical profile analysis from different components of (ZnS-CdS-ZnS)n superlattice wires

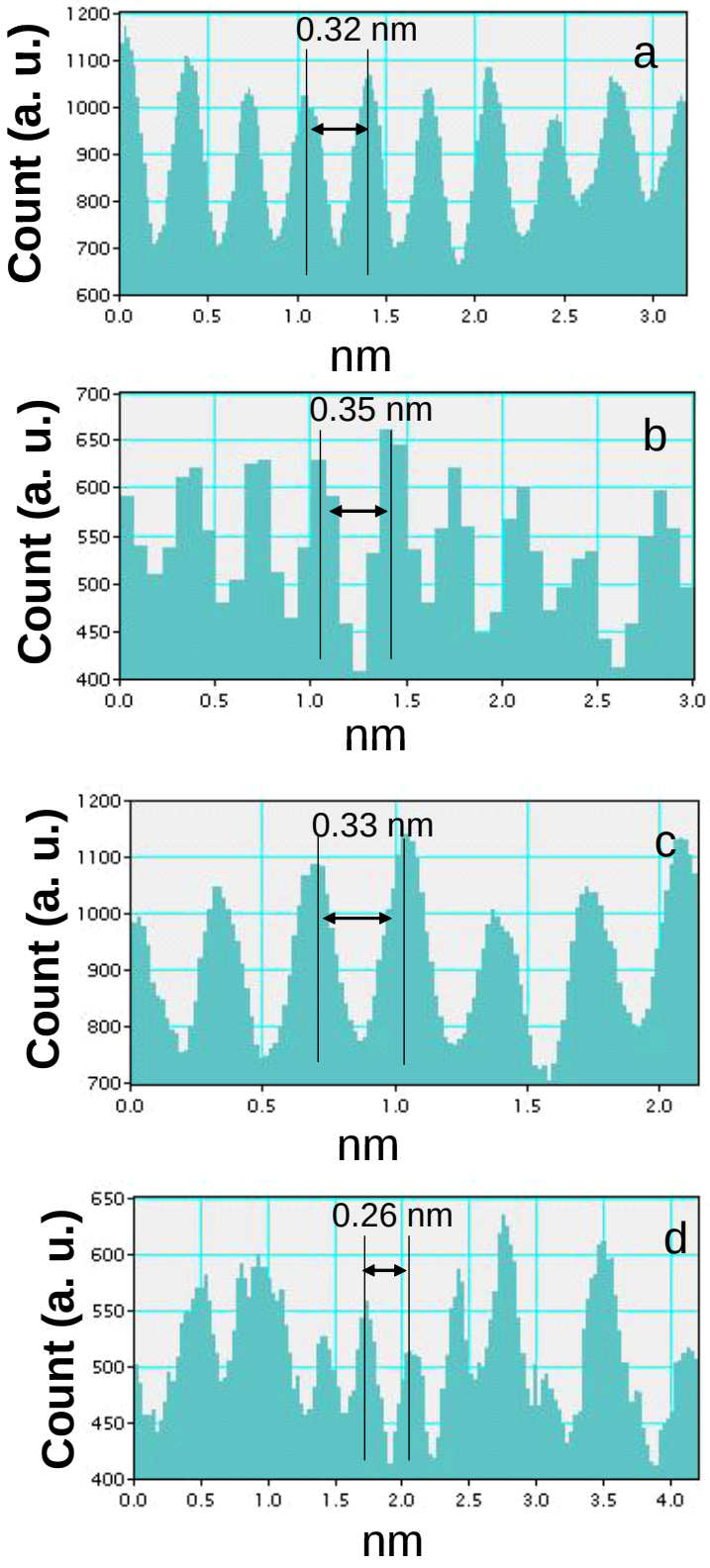

Figure 12. Profile analysis of lattice spacing of (a) ZnS (00.2) planes (b) CdS (10.0) planes (c) CdS (00.2) planes (d) CdS (10.2) planes showing growth of both constituent blocks of the superlattice in wurtzite modifications.

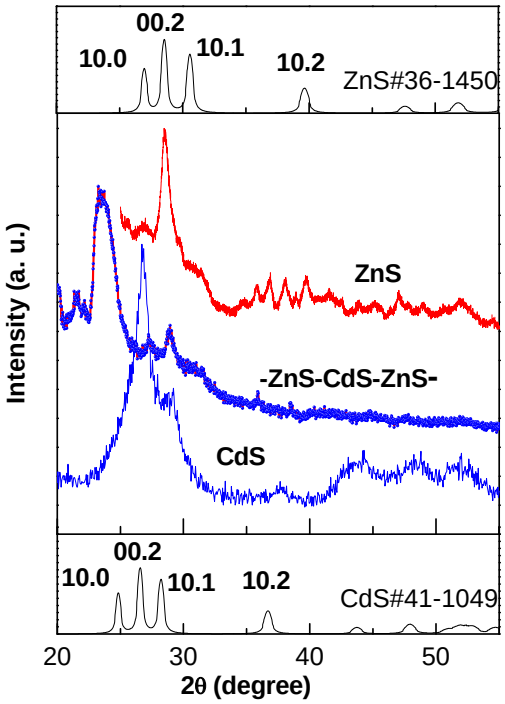

Figure 13. XRD pattern of ZnS rods (red curve), CdS rods as reference structure (blue line) and ZnS-CdS superlattices (red line-blue dots) showing the wurtzite modification of the superlattice wires. The simulated JCPDS patterns show the corresponding peak positions. The ZnS blocks within the heterojunction wire can be indexed to wurtzite ZnS with preferred [001] growth direction. The XRD pattern from CdS blocks also corresponds to the wurtzite phase with [001] preferred orientation along with significant broadening, in agreement with the HRTEM images. The analysis of x-ray line broadening at FWHM of $(002)_{CdSWZ}$ peak by Debye-Scherrer equation from indicates formation of ~1 nm regions of CdS, in line with the proposed model of superlattice wires. The relatively

strong powder diffraction intensity of the (002) planes indicates a greater number of *c*-planes compared to the prismatic planes, which run along the ultranarrow dimension of the elongated structures.

Structure growth Mechanism:

The key parameters in designing ZnS-CdS superlattice system require the 2D supercrystalline nature of ZnS rods which are prone to coalesce into longer wires, use of appropriate amount of Cd-xanthate precursor, and reaction condition tuning. Thermal decomposition of Zn-ethylxanthate in proper reaction conditions yield 2D supercrystalline ZnS rods and wires in (00.2) wurtzite phase.[1] The wurtzite ZnS is intrinsically anisotropic with tetrahedrally coordinated Zn^{+2} and S^{-2} ions stacked alternatively along the c-axis, with the polar basal (00.1) surfaces are truncated exclusively either by S^{-2} anion or by the Zn^{+2} cation resulting in facile formation of rods in the c-direction. The ODA surfactants strongly adsorb to the metal surfaces leaving the anionic S-terminal open. Notably, the end-to-end separation distance between the tips of the nanorods is about half of the side-by-side distance and corresponds to the 2.7 nm length of an upright alkylamine layer. The superstructure domain morphology is consistent with the feature of open S-terminal of the nanorods, as observed in TEM (Figure 1 in this supporting information). We have injected Cd-alkylxanthate at a temperature 70°C above the melting point of ODA, at which the surfactants expectedly remain in molten and dynamic condition. Cadmium chalcogenide nanocrystals can grow anisotropically in the wurtzite modification within the confined spaces provided at the tips of the ZnS nanorods in the presence of amine surfactants.[2,3] The Cd-alkylxanthate

contains a stoichiometric ratio of Cd to S decompose at this temperature,[4] wherein Cd nucleates at the open S terminal of ZnS favored by the electrostatic repulsion between the metal components. The Cd atoms with three dangling bonds on chemically active polar (00.1) facet in wurtzite phase couples with the S terminal of $(00.\bar{1})$ ZnS.[3,5] The nonpolar facets grow at slower rate compared to the basal polar facets restraining the radial growth, and facilitating the CdS nanocrystals to grow preferentially along the $[00\bar{1}]$ direction resulting in bulges of larger diameter within the allowed space available at the tips. The unpassivated S terminal of the resultant CdS unit remains open to couple with the Zn terminal of other ZnS rods while the dynamic ODA stabilizes the structure by adsorbing onto the metal surfaces resulting in periodic units of ZnS connected by CdS regions. Note that we use the four index notation (hk.l) for planes and three index notation [uvw] for directions in the Miller-Bravais hexagonal system (lattice constants *a*, *c* ; lattice angles $\alpha=\beta=90°$, $\gamma=120°$).

As is obvious from the superstructure itself, the uniformity in width is a major controlling factor in the synchronous superlattice formation process, whereas the length of the capping agent affects the interwire spacing. The lattice spacing mismatch of $(10.0)_{CdS}$ and $(00.2)_{CdS}$ with $(00.2)_{ZnS}$ planes are 12.7% and 7.3% respectively. However, the heterojunction wire can tolerate the mismatch by interfacial stain relaxation to grow unidirectionally.[6] The extreme small diameter is also supportive in allowing the anisotropic 1D growth under strain. It stands to reason that a high degree of uniformity is required to achieve the observed pitch registry over large areas. Notably, the thickness of an upright amine layer should approximately be $0.154 + (0.1265 \times 18) + 0.3 = 2.7$ nm, suggesting a center-to-center distance of 6.7 nm for non-penetrating capping layers. The

smaller pitch distance 3.5 nm measured in TEM indicates tilting or interdigitation of capping layers driving the pitch of the assembly, in agreement with the spacing measured by our *in-situ* GI-SAXS measurements on Langmuir trough.[7] The long alkyl chains of the surfactants form interconnected networks wherein the interwire interactions are minimized through short range repulsion and steric hindrance of the surfactant chains.[8] The alkyl groups in the long chain ionic surfactants are apparently more dynamic about the head group (N-C_1 bond), which minimizes along the higher order C_n-C_{n+1} bonds along the alkyl tails.[8] However, the flexibility around the N-C_1 bond increases by increasing alkyl units in the chain length so that the alkyl groups can compact to the minimum energy conformation around the nanowire surface reducing the interwire distance.

UV-vis Absorption Spectroscopy:

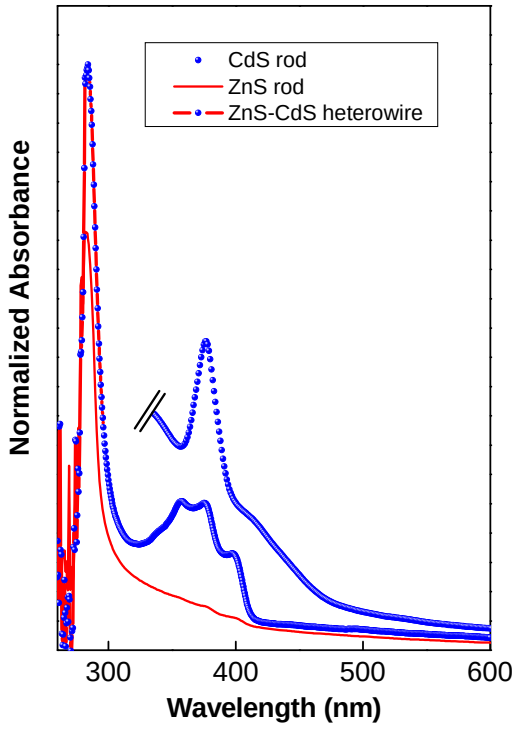

Figure 14. UV-vis absorption of 1.2 nm wide ZnS rods (red curve), 1.7 nm wide CdS reference rods (blue curve) and (ZnS-CdS-ZnS)n superlattices (red line-blue dots) in toluene suspension.

Calculation of CdS particle sizes

We fit the absorption data with the direct band gap using the conventional route

$$\alpha(h\nu) = 2X\ 10^{4}(h\nu - E_g)^{1/2}$$

$$\frac{\alpha^2(h\nu)}{2X10^4} = h\nu - E_g \quad \text{------ (1)}$$

Using equation (1) we obtain the following curve. The extrapolated value of the curve gives an energy of 2.97 eV, which is in extremely good agreement with first transition 420 nm.

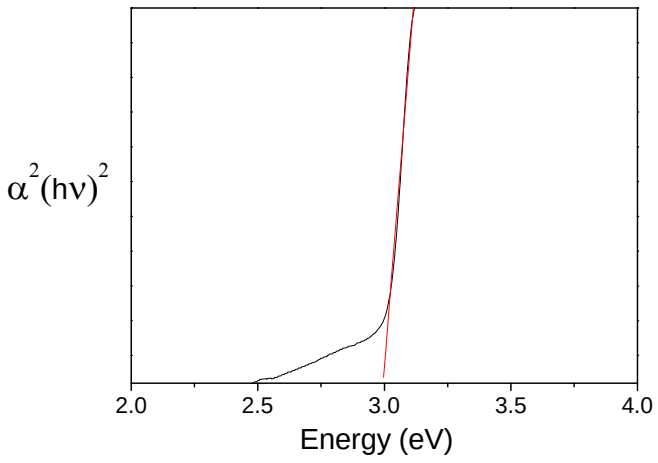

Using this absorption threshold, 2.42 eV bulk band gap, $m_e^* = 0.18$, $m_h^* = 0.53$, the largest CdS size is determined to be 2.2 nm by using the following equation:

$$E_{th} = \left[E_g{}^2 + 2\left(\frac{h}{2\pi}\right)^2 E_g \left(\frac{\pi}{R^2}\right)\left(\frac{1}{m*}\right)\right]^{1/2}$$

where R is the particle of radius, and m* is the effective mass.

References:

[1] Pradhan, N.; Efrima, S. *J. Phys. Chem. B.* **2004**, *108*, 11964.

[2] Milliron, D. J.; Hughes, S. M.; Chi, Y.; Manna, L.; Li, J.; Wang, L-W; Alivisatos, A. P. *Nature*, **2004**, *430*, 190.

[3] Talapin, D. V.; Koeppe, R.; Götzinger, S.; Kornowski, A.; Lupton, J. M.; Rogach, A. L.; Benson, O.; Feldmann, J.; Weller, H. *Nano Lett*. **2003**, *3*, 1677.

[4] Acharya, S.; Patla, I.; Kost, J.; Efrima, S.; Golan, Y. *J. Am. Chem. Soc*., **2006**, *128*, 9294.

[5] Shiang, J. J.; Kadavanich, A. V.; Grubbs, R. K.; Alivisatos, A. P. *J. Phys. Chem.*, **1995**, *99*, 17417.

[6] Talapin, D. V.; Yu, H.; Shevchenko, E, V.; lobo, A.; Murray, C. B. *J. Phys. Chem. C.* **2007**, *111*, 14049

[7] Belman, N.; Acharya, S.; Konovalov, O.; Vorobiev, A.; Israelachvili, J.; Efrima, S.; Golan, Y. *Nano Letters* **2008**, *8*, 3858.

[8] Ji, Q.; Acharya, S.; Hill, J. P.; Richards G. J.; Ariga, K. *Adv. Mat*., **2008**, *20*, 4027.